JOURNAL OF PROPULSION AND POWER
Vol. 17, No. 6, November–December 2001

Upper Bounds on the Flight Speed of Hydrocarbon-Fueled Scramjet-Powered Vehicles

Paul J. Waltrup*
Johns Hopkins University, Applied Physics Laboratory, Laurel, Maryland 20723

Estimates of upper bounds on flight Mach number for scramjet-powered vehicles operating on liquid hydrocarbon fuels assuming either equilibrium or frozen nozzle chemistry are presented. For an axisymmetric missile-shaped vehicle, these upper bounds lie between Mach 9 and 10.

Nomenclature

A	=	area
C_D	=	drag coefficient
C_{Tg}	=	gross engine thrust coefficient
C_{TN}	=	net vehicle force coefficient
ER_e	=	effective fuel-air equivalence ratio
M	=	Mach number
p	=	pressure
q	=	dynamic pressure
α	=	angle of attack
η_c	=	fuel combustion efficiency
η_{KE}	=	inlet kinetic energy efficiency

Subscripts

c	=	combustor
des	=	design
i	=	inlet geometric
max	=	maximum
ref	=	reference
w	=	wall
0	=	freestream
1–5	=	engine stations (see Fig. 1)

Introduction

FROM the inception of the supersonic combustion ramjet (scramjet) engine cycle (see Fig. 1) in the late 1950s through the present time, there has been much speculation about what the upper bound on flight Mach number is when using either a gaseous fuel such as hydrogen or a storable liquid hydrocarbon fuel such as kerosene. Some initial studies claimed orbital speeds (Mach 26) and beyond for hydrogen-fueled systems and Mach 14–16 flight for hydrocarbon-fueled systems.[1–3] Subsequent studies in the 1960s and early 1970s revised these estimates downward somewhat to Mach 15–20 and Mach 12–14,[4–7] respectively. However, most of these studies are not configuration specific, and none incorporate what has been learned about the operation and performance of scramjet-powered vehicles since their printing.

Subsequent to these early studies, several modern studies have been done for hydrogen-fueled concepts, primarily for Earth-to-orbit space transport systems,[8–11] in which the upper speed bound is somewhat lower, primarily in the Mach 12–16 range. There have also been a number of studies on hydrocarbon-fueled missile concepts,[12–16] but none of these addressed the upper Mach number limit. The purpose of this paper is to present a modern, systematic approach to reestablishing these limits for hydrocarbon-fueled vehicles and to provide a representative example for reference.

Upper Bound(s) on Flight Mach Number

The approach used to establish the upper bounds on flight Mach number was to conduct performance sensitivity studies on a liquid hydrocarbon-fueled scramjet-powered missile based on the known physics and chemistry of scramjet engines and their requisite energy balance with the vehicle's structure. The engine cycle analysis code used was RJPA,[17] the current U.S. industry standard for scramjet engines. To keep the initial computational matrix to a manageable level, only an axisymmetric nose inlet scramjet engine/missile configuration was considered,[18,19] as shown in Fig. 1. Any other engine configuration, for example, aft-mounted engine, underslung engine, podded engine(s), etc., would have lower thrust performance, primarily because of lower air capture and, therefore, a lower upper bound on flight Mach number.

It was also assumed that the inlet design Mach number was the same as the flight Mach number (a variable geometry inlet) to maximize thrust at these high flight speeds and that the vehicle flew at a constant dynamic pressure q_0 equal to 47.88 MN/m^2 (1000 lbf/ft^2). The bounds on inlet area contraction chosen are also based on work with variable geometry inlets[20] and, therefore, representative of the upper limits on inlet area contraction (and thrust generation) for all flight speeds. The corresponding inlet kinetic energy efficiencies as a function of flight speed and area contraction were also obtained from Ref. 20.

JP-7 endothermic liquid hydrocarbon fuel was chosen rather than RJ-5 as used in Refs. 12, 18, and 19 because such a fuel will likely be required for structural cooling at flight Mach numbers above 6.5. For simplicity, it was assumed that any engine structural cooling required was accomplished with the engine fuel flow, the net effect on the energy balance being zero. Here, it is assumed that the energy transferred to the fuel during structural cooling exactly equals the energy added to the fuel before its injection in the combustor. Although this would not be the exact case in an actual engine or flight vehicle, it is representative of what happens in an engine, that is, any energy extracted from the engine's structure via fuel cooling to maintain its integrity will end up being injected into the combustor (or the exit nozzle if the cooling fuel flow rate is higher than that required by the engine). The best circumstance is when all of the heated fuel is injected into the combustor, resulting in a nearly adiabatic energy extraction and addition process. Any influence on engine performance other than this is beyond the scope of the current study.

The remainder of the reference engine and vehicle geometry (other than the inlet) is as described in Ref. 18, that is, the missile maximum diameter is 50 cm, reference area A_{ref} is 1963.5 cm^2, and missile length is 400 cm. The engine inlet[19] is $A_0 = A_i$ when $\alpha = 0$ deg. For $M_0 = 8$, 9, 10, 11, and 12, $(A_i/A_2)_{max} = 12.278$, 13.922, 15.500, 17.002, and 18.428, whereas $\eta_{KE} = 0.9662$, 0.9673, 0.9700, 0.9722, and 0.9740. The cowl angle is 6 deg, the isolator L/D is 10, the combustor area ratio is 4, the combustor wall area

Received 22 February 2001; revision received 5 August 2001; accepted for publication 5 August 2001. Copyright © 2001 by the American Institute of Aeronautics and Astronautics, Inc. Under the copyright claimed herein, the U.S. Government has a royalty-free license to exercise all rights for Governmental purposes. JHU/APL reserves all proprietary rights other than copyright; the author(s) retain the right of use in future works of their own; and JHU/APL reserves the right to make copies for its own use, but not for sale. All other rights are reserved by the copyright owner.

*Senior Engineer/Scientist. Associate Fellow AIAA.

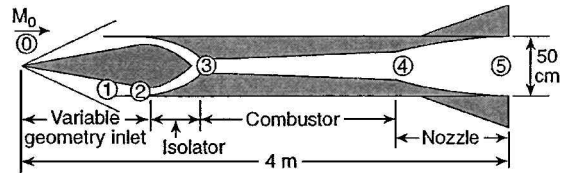

Fig. 1 Schematic of axisymmetric, scramjet-powered missile.

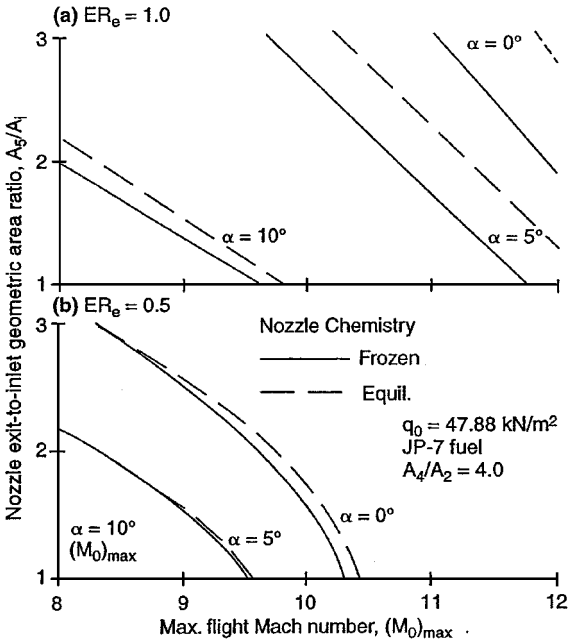

Fig. 2 $(M_0)_{max}$ plotted against nozzle exit-to-inlet geometric area ratio A_5/A_i for different values of α.

is $40A_2$, and the combustion efficiency η_c is 100%. The effective equivalence ratio ER_e is 0.5, 1.0, the inlet and combustor chemistry are in equilibrium, the nozzle efficiency is 0.98, and the nozzle chemistry is in equilibrium or frozen.

Sensitivity studies were then performed wherein gross engine thrust coefficient C_{tg} was computed as a function of these inputs using the following parametric variations: inlet η_{KE} is ± 0.01 from the nominal, inlet A_i/A_2 is nominal to -35% of the nominal, and combustor A_4/A_2 is 1–4. The fuel is JP-5, RJ-5, and ethylene, the nozzle A_5/A_i is 1–3, and the angle of attack α is 0, 5, and 10 deg. Previous studies have established the performance sensitivity of the engine to other variations in geometry and component efficiencies.[12,18]

The resulting engine performance was plotted as a function of M_0 and total vehicle drag coefficient C_D, with the flight Mach number at which the two curves cross defined as the maximum flight Mach number $(M_0)_{max}$. These curves are presented in the Appendix for reference. Note that fuel temperature (or enthalpy) is not among the variables investigated because as discussed earlier, the energy used to heat the fuel would have come from energy extracted from the engine's structure to maintain its integrity, and the net effect on engine performance (other than enhancing the ability of the fuel to ignite and burn) is essentially nil.

The results are given in Figs. 2–6 wherein the Mach number at which the net thrust coefficient of the engine and vehicle equals the vehicle's external drag is plotted against the sensitivity parameter. Here, the vehicle external drags are those presented in Ref. 18 or an extension thereof from Mach 8 to 12. Included in each plot are the $ER_e = 0.5$ and 1.0 engine performance curves for both equilibrium and frozen flow in the exit nozzle.

In Fig. 2, the influence of A_5/A_i on $(M_0)_{max}$ is presented for all three angles of attack. Note that in all cases, the value of $(M_0)_{max}$ for frozen nozzle flow is less than or equal to that for equilibrium nozzle flow. Because the nozzle chemistry at these flight speeds will be assumed to be frozen, subsequent discussions will be focused on the frozen chemistry results. The results show that for $ER_e = 1.0$, the maximum flight Mach number experiences a substantive drop (about

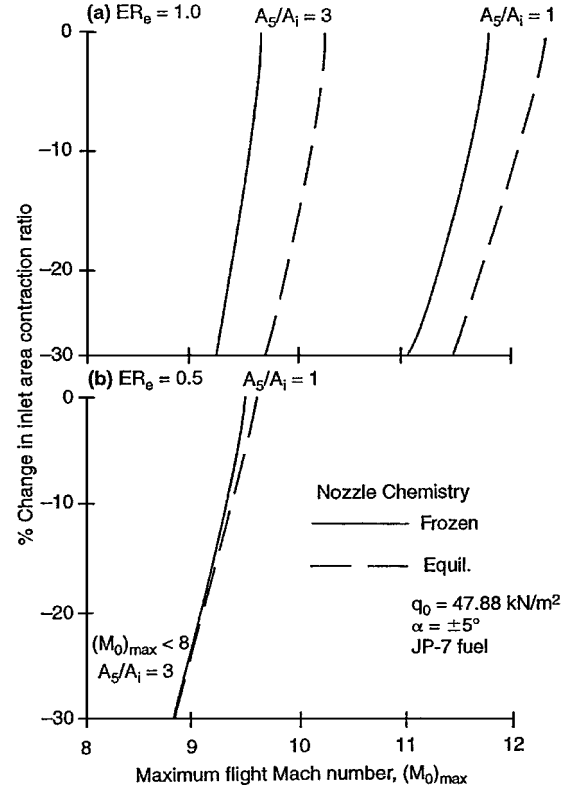

Fig. 3 $(M_0)_{max}$ plotted against inlet contraction.

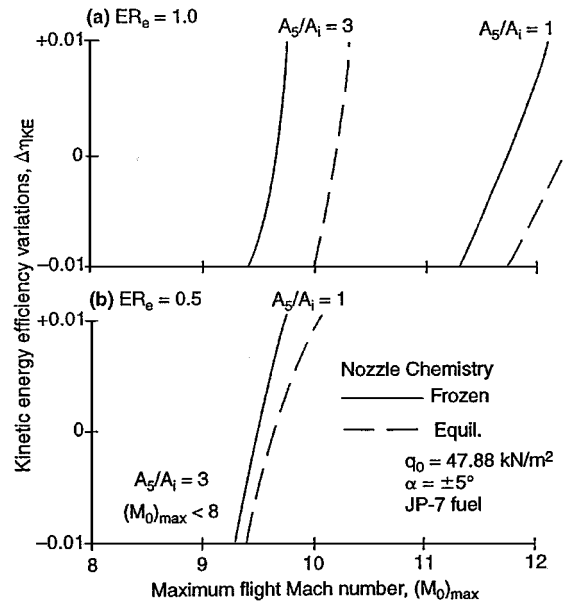

Fig. 4 $(M_0)_{max}$ plotted against inlet efficiency variations.

2 Mach numbers) as A_5/A_i increases from 1 to 3 for $\alpha = \pm 5$ deg with a similar trend at the other two values of α. Here, $(M_0)_{max}$ decreases from 11.75 to 9.65 for $\alpha = \pm 5$ deg. When $\alpha = 0$ deg, $(M_0)_{max}$ is 11 or greater. However, when $\alpha = 10$ deg, $(M_0)_{max}$ is 9.6 or less, falling below Mach 8 for $A_5/A_i > 2$.

A similar trend is noted for $ER_e = 0.5$ as well, although the absolute values of $(M_0)_{max}$ are substantially lower. For $\alpha = 0$ deg, $(M_0)_{max}$ drops from 10.3 to 8.3 as A_5/A_i increases from 1 to 3, and at $\alpha = \pm 5$ deg, it drops from a maximum value of 9.5 when $A_5/A_i = 1$ to below 8 when A_5/A_i exceeds 2.15. For $\alpha = \pm 10$ deg, $(M_0)_{max}$ is always less than 8.

What does all of this mean? First, when $ER_e = 1.0$, the vehicle will have no additional axial acceleration capabilities, and so the values of $(M_0)_{max}$ are just that, absolute maximums. If acceleration capabilities are desired or required (as they almost always are) at

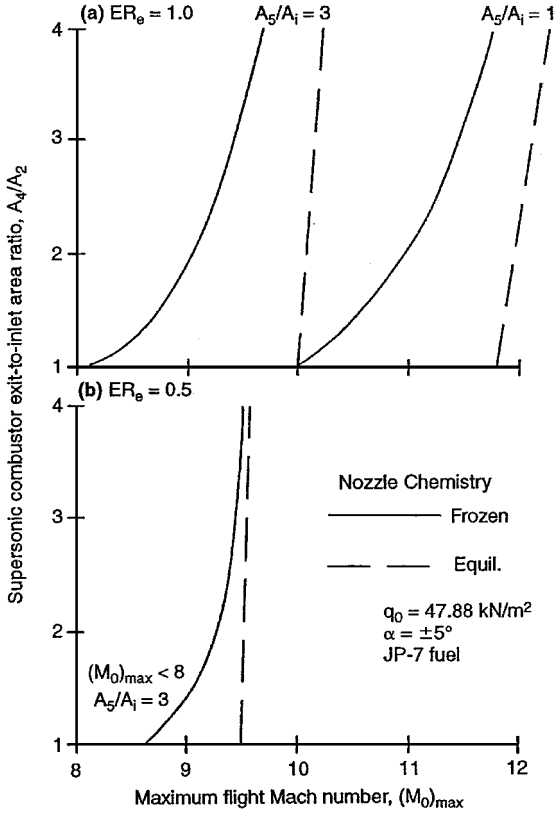

Fig. 5 $(M_0)_{max}$ plotted against combustor area ratio.

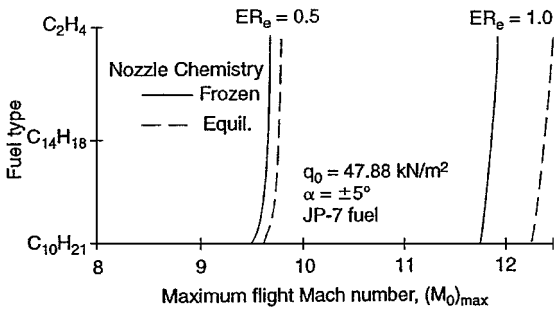

Fig. 6 $(M_0)_{max}$ plotted against fuel type.

these flight speeds, then a reduced ER_e is necessary. In this study, the lower bound on this reduced ER_e is assumed to be 0.5. Furthermore, for the altitudes of interest in these studies (>30 km), the vehicle will require an angle of attack of 5 deg or greater to cruise, and so the $\alpha = 0$ deg results are not applicable unless a ballistic trajectory is commanded, a highly unlikely scenario because this is an airbreathing engine. As a consequence, the maximum Mach number curves applicable to this vehicle when cruising at a dynamic pressure of 47.88 MN/m^2 are those bounded by $ER_e = 0.5$ and 1.0 and $\alpha = \pm 5$ deg.

Although these arguments compress the bounds on $(M_0)_{max}$, there is still a substantial spread. For example, for $A_5/A_i = 1$, the maximum flight Mach number will vary between 9.5 and 11.75, the choice depending on the acceleration capability desired. Note that engine thrust and fuel specific impulse I_{sp} exhibit opposing trends with the value of A_5/A_i. The lower the value of A_5/A_i is, the higher the absolute value of thrust (for a fixed nozzle exit area) because of an increase in the amount of air captured by the engine. The opposite is true, however, for I_{sp}. As a result, an engine with a high I_{sp} may well have a low thrust and vice versa. These trends are apparent in the curves of Fig. 2, wherein the maximum Mach number decreases with increasing A_5/A_i because of decreasing engine thrust. Ultimately, the actual value of $(M_0)_{max}$ will depend on the specific vehicle design and mission range and acceleration requirements. Because of this dichotomy, subsequent sensitivity curves are presented for $\alpha = \pm 5$ deg and two values of A_5/A_i, 1 and 3.

Figure 3 presents the sensitivity of $(M_0)_{max}$ to decreases in the inlet area contraction ratio given earlier (increase in the inlet throat area A_2). The result indicates that $(M_0)_{max}$ is not very sensitive to increases in the inlet throat area, irrespective of the value of A_5/A_i, at least in the 0–30% range investigated herein. For $ER_e = 1$, $(M_0)_{max}$ decreases from 11.75 to 11.05 with a 30% increase in the inlet throat area A_2 with $A_5/A_i = 1.0$. When $A_5/A_i = 3.0$, $(M_0)_{max}$ decreases from 9.65 to 9.25. For $ER_e = 0.5$ and $A_5/A_i = 1.0$, $(M_0)_{max}$ decreases from 9.5 to 8.8. For $A_5/A_i = 3.0$, $(M_0)_{max}$ is always less than 8.

Figure 4 presents the corresponding curves for a ± 0.01 variation in inlet kinetic energy efficiency η_{KE}. These results show that $(M_0)_{max}$ is not sensitive to large changes in inlet pressure recovery, at least at the flight speeds of interest. When ER_e and $A_5/A_i = 1.0$, a ± 0.01 change in η_{KE} only changes $(M_0)_{max}$ by $+0.35$ and -0.45, respectively, ranging in value from 12.1 to 11.3. When $A_5/A_i = 3.0$, the range is from 9.75 to 9.4, respectively, and when $ER_e = 0.5$ and $A_5/A_i = 1.0$, the range is from 9.75 to 9.3, respectively. $(M_0)_{max}$ is always less than 8 when $ER_e = 0.5$ and $A_5/A_i = 3.0$.

Figure 5 presents the sensitivity of $(M_0)_{max}$ to combustor area ratio A_4/A_2. The sensitivity of $(M_0)_{max}$ to changes in combustor area ratio is large and on the same order of magnitude as its sensitivity to A_5/A_i for frozen nozzle chemistry. For the cases studied with $ER_e = 1.0$, $(M_0)_{max}$ varies from 11.75 when $A_4/A_2 = 4$ to 10 for a constant area combustor for $A_5/A_i = 1$. The respective values when $A_5/A_i = 3$ are 9.65 and 8.1. When $ER_e = 0.5$, $(M_0)_{max}$ varies between 9.5 and 8.6 when $A_5/A_i = 1$ (about 50% of the variation at $ER_e = 1$) and is always less than 8 when $A_5/A_i = 3$.

Why is there this sensitivity to combustor and nozzle exit area ratio? It is because of the influence of the type of kinetics in the exit nozzle. The larger the area expansion in the exit nozzle is, the stronger the influence of frozen chemistry on engine performance. For example, for a fixed exit nozzle area, a low value of combustor area ratio will result in a larger nozzle exit-to-combustor exit area expansion than for a larger combustor exit area (or combustor area ratio). This, in turn, results in more of the total nozzle exit-to-combustor inlet area expansion taking place in the nozzle when the chemistry is nearly frozen, as compared to the expansion taking place in the combustor, where the chemistry is assumed to be in equilibrium.

As a result, care must be taken in the amount of area expansion permitted (or assumed) in the combustor when performing engine cycle performance calculations such as those in this (or any previous) study. Because the total area expansion between the combustor entrance and nozzle exit can be assigned to either the combustor or exit nozzle, and equilibrium chemistry is assumed in the combustor and frozen chemistry in the exit nozzle, quite different engine and vehicle performance estimates can be computed for the same engine configuration depending on where this area expansion (and, therefore, type of chemistry) is assumed to take place. For example, the limits shown in Figs. 2–6 would move to the left as less area expansion is taken in the combustor (less energy is available for thrust, it is tied up in dissociated chemical species) and to the right as the combustor area ratio approaches the total area expansion available.

Consequently, care must be exercised as to where the total combustor-plus-exit nozzle area expansion is taken. Remember that the assumption of equilibrium chemistry in the combustor is based on a low-to-moderate area expansion in the combustor. Otherwise, the actual combustor exit chemistry will move away from equilibrium and toward frozen flow. As a result, an upper bound on A_4/A_2 of 4 was taken for this study.

The last set of sensitivity curves are for the type of hydrocarbon fuel used in the engine. As shown in Fig. 6, $(M_0)_{max}$ is quite insensitive to the type of fuel used, irrespective of ER_e, for $A_5/A_i = 1.0$. Here, RJ-5 is a dense (specific gravity = 1.08) storable hydrocarbon, JP-7 is a lighter (specific gravity < 0.8) storable endothermic hydrocarbon, and ethylene (C_2H_4) is a light gaseous hydrocarbon and one of the endothermic decomposition products of JP-7. Because these

same trends (with lower absolute values) are valid for other values of A_5/A_i, they are not included for brevity.

Finally, if one were to limit the value of ER_e to 0.5, it is possible to set a more precise (and also reasonable) bound on $(M_0)_{\max}$. If this hypothesis is accepted, the maximum flight Mach number of a hydrocarbon-fueled scramjet-powered vehicle flying a $q_0 = 47.88$ MN/m^2 trajectory would be between Mach 9 and 10.

Conclusions

To summarize, a reasonable upper bound on flight Mach number would appear to be between Mach 9 and 10, but the precise value is a strong function of the vehicle design and mission acceleration and cruise range requirements. The upper bound is most sensitive to variations in the nozzle exit-to-diffuser-inletand combustor area ratios and much less sensitive to inlet area contraction and inlet efficiency. It is very insensitive to the type of hydrocarbon fuel used, but range and other systems considerations may be quite sensitive to the fuel type.

Appendix: Scramjet Performance Curves for Determination of Maximum Flight Mach Number (Figs. A1–A7)

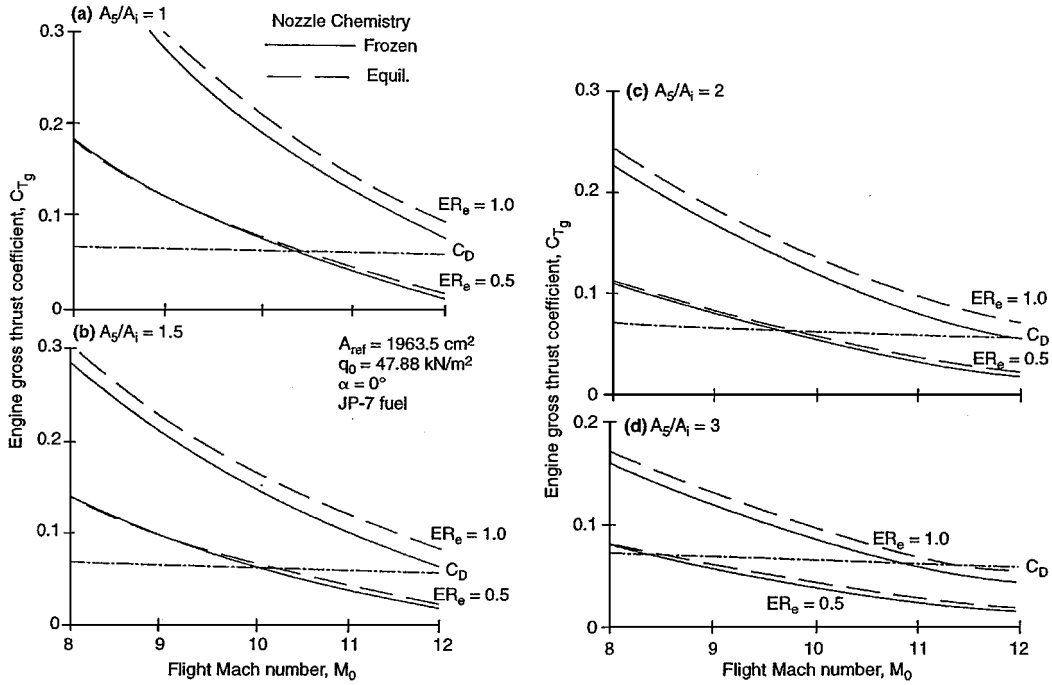

Fig. A1 Engine gross thrust as a function of flight Mach number for $\alpha = 0$ deg.

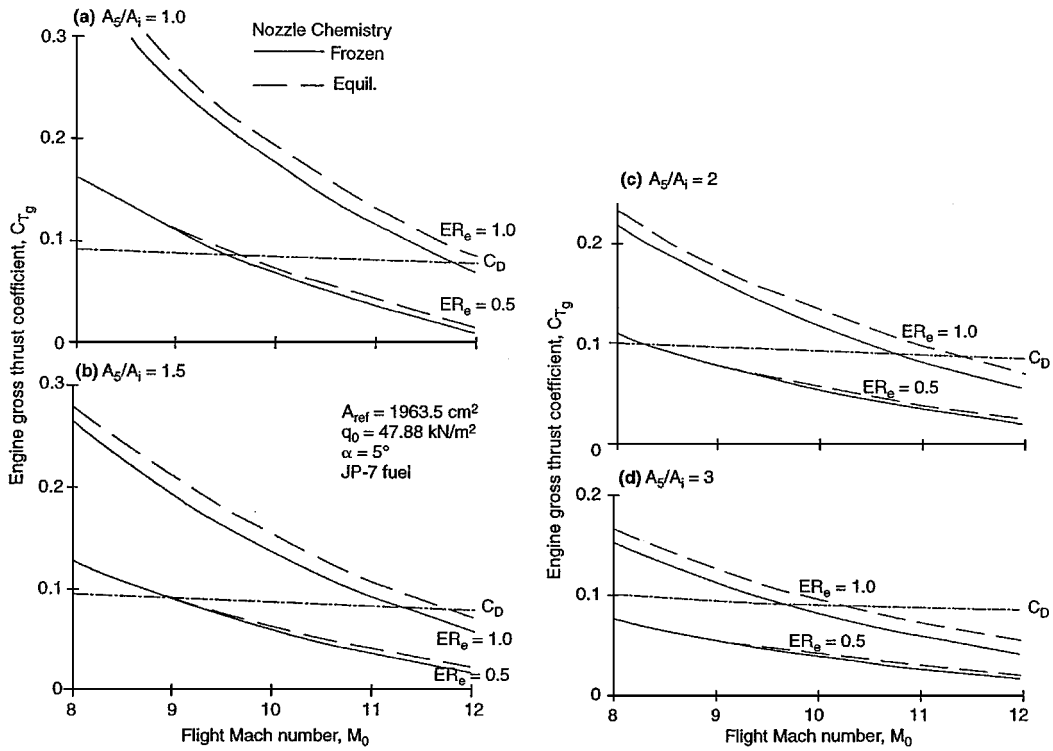

Fig. A2 Engine gross thrust as a function of flight Mach number for $\alpha = 5$ deg.

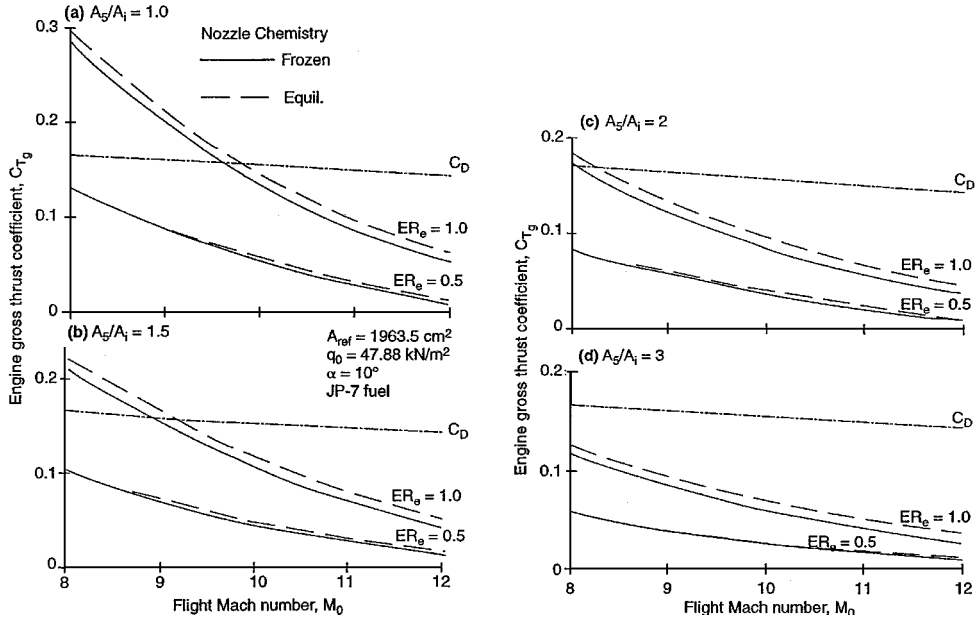

Fig. A3 Engine gross thrust as a function of flight Mach number for $\alpha = 10$ deg.

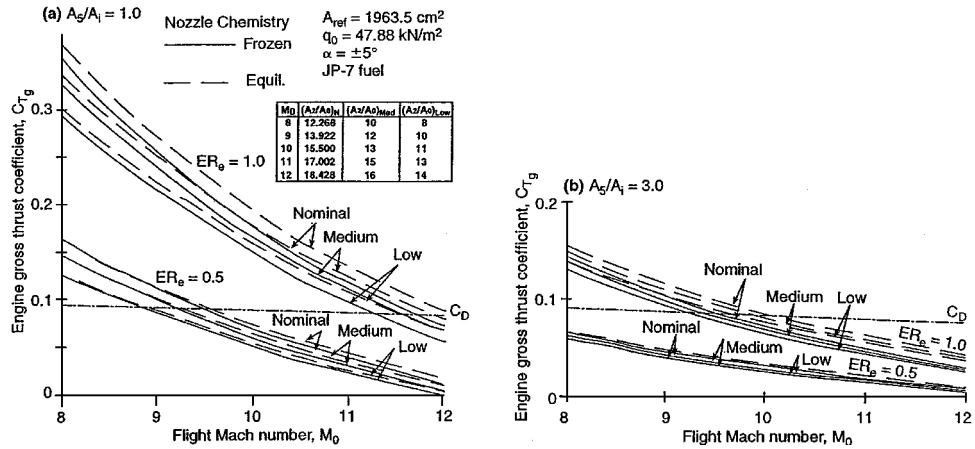

Fig. A4 Effect of inlet area contraction on engine gross thrust at $\alpha = 5$ deg.

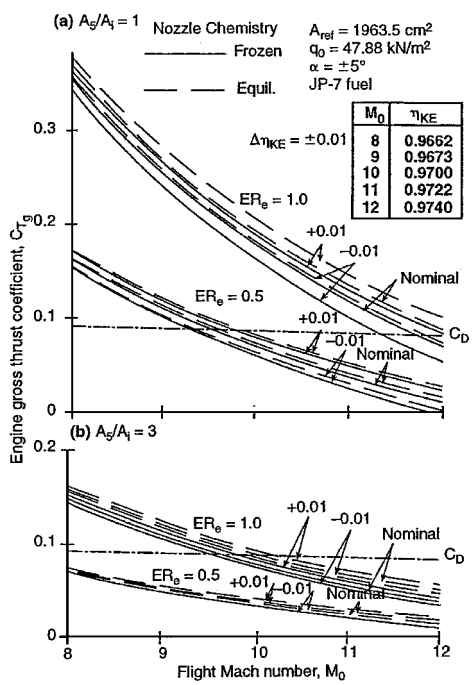

Fig. A5 Effect of inlet kinetic energy efficiency on engine gross thrust at $\alpha = 5$ deg.

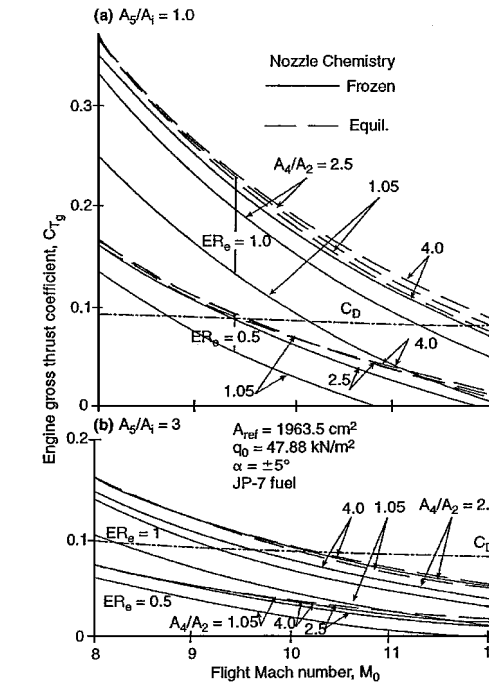

Fig. A6 Effect of combustor area ration on engine gross thrust at $\alpha = 5$ deg.

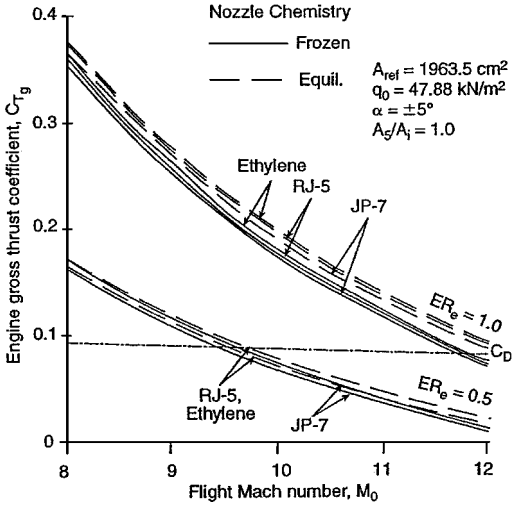

Fig. A7 Effect of fuel type on engine gross thrust at $\alpha = 5$ deg.

References

[1]*Proceedings of the Fourth AGARD Colloquium*, Milan, Italy (Permagon Press, New York), 1960.

[2]*Combustion and Propulsion–High Mach Number Air Breathing Engines*, Permagon Press, New York, 1960.

[3]Weber, R. J., and McKay, J. S., "An Analysis of Ramjet Engines Using Supersonic Combustion," NACA TN-4386, 1958.

[4]Hawkins, R., and Fox, M. D., "An Investigation of Real Gas Effects Relevant to the Performance of a Kerosene Fueled Hypersonic Ramjet," *Supersonic Flow, Chemical Processes and Radiative Transfer,* edited by X. Olfe and Y. Zakkay, MacMillan, New York, 1964, pp. 113–135.

[5]Swithenbank, J., and Parsons, R. J., "Experimental Techniques for Supersonic Combustion Research in a Shock Tunnel," NATO/AGARD Rept. 95, Sept. 1967.

[6]Payne, R., "Supersonic Combustion of Liquid Kerosene," AFOSR-TR-75-0865, April 1975.

[7]Curran, E. T., and Stull, F. D., "The Potential Performance of the Supersonic Combustion Ramjet Engine," Aeronautical Systems Div., Rept. ASD-TDR-63-336, U.S. Air Force, Wright–Patterson AFB, OH, May 1963.

[8]Chase, R. L., and Tang, M. H., "A History of the NASP Program from the Formation of the Joint Program Office to the Termination of the HySTP Scramjet Performance Demonstration Program," AIAA Paper 95-6031, April 1995.

[9]Kobayashi, S., and Maita, M., "Japanese Spaceplane Program Overview," AIAA Paper 95-6002, April 1995.

[10]Falempin, F., Lacaze, H., Wagner, A., and Viala, P., "Reference and Generic Vehicle for the French Hypersonic Technology Program," AIAA Paper 65-6008, April 1995.

[11]Sosounov, V., "High Velocity Flight Propulsion: Scientific Study and Achievement," Seminar, Arnold AFB, TN, Sept. 1997.

[12]Waltrup, P. J., "The Dual Combustor Ramjet: A Versatile Propulsion System for Hypersonic Tactical Missile Applications," CP-526, AGARD Paper 8, Sept. 1992.

[13]Kay, I. W., Peschke, W. T., and Guile, R. N., "Hydrocarbon-Fueled Scramjet Combustor Investigation," *Journal of Spacecraft and Rockets*, Vol. 8, No. 2, 1992, pp. 507–512; also AIAA Paper 90-2337, June 1990.

[14]Andrews, E. H., Trexler, C. A., and Emami, S., "Tests of a Fixed-Geometry Inlet–Combustor Configuration for a Hydrocarbon-Fueled Dual-Mode Scramjet," AIAA Paper 94-2817, June 1994.

[15]Bulman, M. J., and Siebenhaar, A., "The Strutjet Engine: Exploding the Myths Surrounding High Speed Airbreathing Propulsion," AIAA Paper 95-2475, July 1995.

[16]Mercier, R. A., and Ronald, T. M. F., "Hypersonic Technology (HyTech) Program," AIAA Paper 97-7027, Sept. 1997.

[17]Pandolfini, P. P., and Friedman, M. A., "Instructions for Using Ramjet Performance Analysis (RJPA) IBM-PC Version 1.24," Applied Physics Lab., Rept. JHU/APL AL-92-P175, Johns Hopkins Univ., Laurel, MD, June 1992.

[18]Waltrup, P. J., Billig, F. S., and Stockbridge, R. D., "Engine Sizing and Integration Techniques for Hypersonic Airbreathing Missile Applications," CP-307, AGARD, Paper 8, March 1982.

[19]Billig, F. S., Corda, S., and Pandolfini, P. P., "Design Techniques for Dual Mode Ram–Scramjet Combustors," CP-479, AGARD, June 1990.

[20]Billig, F. S., Waltrup, P. J., Gilreath, H. E., White, M. E., Van Wie, D. M., and Pandolfini, P. P., "Proposed Supplement to the Proposed Propulsion System Management Support Plan," Applied Physics Lab., Rept. JHU/APL-NASP 6-1, Johns Hopkins Univ., Laurel, MD, July 1986.